université paris – sud
INSTITUT DE PHYSIQUE NUCLEAIRE
B.P. N° 1 – 91406 - ORSAY – TEL. 941.51.10
laboratoire associé à l'IN2P3

PRODUCTION OF ^{149}Tb IN DEEP INELASTIC TRANSFER REACTIONS : AN APPROACH TO THE ANGULAR MOMENTUM OF FRAGMENTS

M.F. Rivet, R. Bimbot and D. Gardès
I.P.N. Orsay

and

A. Fleury, F. Hubert and Y. Llabador
C.E.N. Bordeaux-Gradignan

IPNO-RC-78-06

Soumis à Z. für Physik

PRODUCTION OF ^{149g}Tb IN DEEP INELASTIC TRANSFER REACTIONS : AN APPROACH TO THE ANGULAR MOMENTUM OF FRAGMENTS.

M.F. Rivet, R. Bimbot and D. Gardès
I.P.N. Orsay

and

A. Fleury, F. Hubert and Y. Llabador
C.E.N. Bordeaux-Gradignan

-:-:-:-

Abstract : The excitation functions for deep inelastic reactions in which two to six charges are transferred from ^{40}Ar and ^{63}Cu ions to rare earth targets have been measured using activation techniques, the observed radionuclides being ^{150,151}Dy and ^{149g}Tb. From the comparison of the curves relative to ^{149g}Tb and those relative to ^{150,151}Dy, it was deduced that the low spin isomer ^{149g}Tb was produced with significant probability for low incident energies. Using data from (heavy ions,xn) reactions, it was possible to attribute this production to the deexcitation of Tb fragments formed in deep inelastic transfers with angular momenta lower than 9 ħ. This result is in good agreement with the angular momentum calculations performed under the hypothesis that the initial angular momentum window leading to deep inelastic reactions is situated between the critical angular momentum for fusion and that corresponding to grazing collisions. As far as Cu induced reactions are concerned, both hypothesis of rolling and sticking are consistent with the experimental data. For Ar induced reactions, the results indicate that the stage of sticking is not reached when the incident energy is lower than 200 MeV.

Keyword Abstract :

NUCLEAR REACTIONS : $^{142,145}Nd$, $^{144,148}Sm$, $^{154}Gd(Ar,X)^{151,150}Dy$, ^{149g}Tb E = 160-280 MeV ; measured σ (E). ^{144}Nd, ^{148}Sm, ^{151}Eu, $^{154}Gd(Cu,X)^{151,150}Dy$, ^{149g}Tb. E = 280-420 MeV measured σ(E). Enriched targets. Deduced angular momentum of Tb fragments.

I - INTRODUCTION

One of the rather unknown features of deep inelastic transfer reactions (D.I.T.) is the part of the initial angular momentum which is transformed into intrinsic angular momentum of the fragments. Experimentally this quantity is difficult to reach. It can be estimated from the measurement of γ multiplicities associated with each light DIT residue[1-3]. But the interpretation of such data is not easy, because two assumptions must be made in order to deduce the fragment angular momenta : one concerns the average number of $\hbar$ units carried away be each γ transition, the second concerns the angular momentum removed by particle evaporation. For reactions induced in heavy targets (like Bi), the sequential fission of the heavy fragment can also be used to estimate the average angular momentum transfer in DIT[4]. Other methods, such as the analysis of the fragment kinetic energy variation versus incident energy[5], and the study of the nuclear polarization through the measurement of the circular polarization of γ rays emitted by the excited fragment[6] or through that of the angular distribution of β rays from the residual nucleus[7] have also be used to investigate the problem of angular momentum transfers in D.I.T. reactions.

The present work is another approach to this problem, which consists in studying the heavy fragment angular momentum through the production yield of a low spin isomer ^{149g}Tb : Deep inelastic reactions in which two to six charges are transferred from Ar and Cu ions to rare earth targets have been studied by observing the heavy residues ^{151}Dy, ^{150}Dy and ^{149g}Tb, these nuclei being identified by their α-radioactivity as in refs[8-10]. The corresponding excitation functions have been measured and compared to each other. The curves relative to ^{149g}Tb exhibit a low energy structure which does not appear for those relative to ^{150,151}Dy. This enhancement of the cross section at low energy is attributed to the direct production of ^{149g}Tb, whereas, for higher energies, the main contribution to the observed cross section is the electron capture decay of ^{149}Dy. It was shown in a previous study by Alexander and Simonoff[11] that, because of the presence of a high spin isomer ^{149m}Tb($J=\frac{11}{2}$), such direct production of the low spin isomer ^{149g}Tb($J=\frac{5}{2}$) through evaporation from an excited Tb compound nucleus is possible only if this excited nucleus has a low angular momentum ($\lesssim 9\,\hbar$). Therefore, the observation of ^{149g}Tb directly produced through D.I.T. reactions may be interpreted as an evidence for the existence of primary fragments with angular momenta lower than $9\,\hbar$.

II - EXPERIMENTAL EVIDENCE FOR ^{149g}Tb PRODUCTION

II.1. Experimental technique

The excitation functions of ^{150,151}Dy and ^{149g}Tb produced by deep inelastic reactions have been measured using activation techniques as described in ref.[8-10]. The projectiles used, ^{40}Ar and ^{63}Cu, were accelerated with the Orsay ALICE facility. The rare earth target and a stack of Al catcher foils were placed inside a Faraday cup. During the irradiations, the integrated beam was carefully measured, and the intensity variations were recorded to be taken into account in the cross section calculations. The α-activities of the catcher foils and target were counted off-line in 2π ionization chambers. The decay characteristics are given in table 1. The beam energy E_{lab} was calculated from the cyclotron parameters (frequency F and extraction radius R), using the relation $E = \frac{F^2R^2}{4.84} A$ (1), (A being the ion mass) with a correction of - 1.3 % to take into account the systematic deviations observed between the measured and calculated energies[12]. When Al degraders were used, the energy was calculated from the recent measurements of Bimbot et al.[13]. Thus the overall uncertainty in the incident energy was of the order of ± 2·3 %.

II.2. Excitation functions for ^{151}Dy, ^{150}Dy and ^{149g}Tb production

The cross sections for the production of ^{150,151}Dy and ^{149g}Tb have been measured for the reactions induced by ^{40}Ar in targets of ^{142,145}Nd, ^{144,148}Sm and ^{154}Gd and for reactions induced by ^{63}Cu in ^{144}Nd, ^{148}Sm, ^{151}Eu and ^{154}Gd. For each of these targets, the nature of the transfer reaction leading to the observed isotopes is given in table 2, expressed as the net gain of nucleons by the target. As was already discussed in ref.[8-10], these numbers must be taken as the final result of a two step reaction, a transfer of nucleons followed by nuclear evaporation. It should be noticed from table 2 that all the reactions studied involve the transfer and/or evaporation of a significant number of nucleons. Moreover, the measured angular and energetic distributions of the reaction products published in ref.[8-10,14] are typical of deep inelastic reactions. The cross sections measured for each of these reactions are given in tables 3 and 4. The errors on σ quoted in these tables include the uncertainties in the counting rates (± 1 % to ± 30 %), target thicknesses (± 12 %), branching ratios (see table 1), counting efficiencies and self-absorption of α particles in the catcher foils (± 5 %).

The excitation functions for the reactions induced in ^{144}Sm by ^{40}Ar are plotted in fig. 1. It can be seen from this graph that the curves corresponding to the production of ^{151}Dy and ^{150}Dy exhibit a similar behavior, with a permanent increase all over the energy range, and a trend to level off at high energies. The excitation function for ^{149g}Tb production is completely different : the high energy plateau is similar to the previous ones, but the excitation function exhibits a low energy structure which is not observed for the curves relative to ^{150}Dy and ^{151}Dy. This experimental fact can be explained as follows : First is should be noted that, because of the relatively fast electron capture decay of $^{150,151}Ho$, $^{150,151}Er$, the measured cross sections $\sigma(^{150}Dy)$ and $\sigma(^{151}Dy)$ are cumulative yields. For the same reason, the measured ^{149g}Tb cross section can be written as the sum of two terms :

$$\sigma(^{149g}Tb) = \sigma_d(^{149g}Tb) + r\,\sigma(^{149}Dy) \qquad (2)$$

where the first term represents the direct production of cold ^{149g}Tb nuclei, and the second one the production of ^{149g}Tb through radioactive decay of ^{149}Dy by electron capture. The symbol r is the electron capture branching ratio of ^{149}Dy ($r = 0,475$ [16]) and $\sigma(^{149}Dy)$ the cumulative yield for ^{149}Dy. Therefore, the ^{149g}Tb excitation functions includes the additional component $\sigma_d(^{149g}Tb)$ relative to those of ^{150}Dy and ^{151}Dy. The second term in equation 2 can be estimated from the other Dy excitation functions : it can be seen in fig. 1 that, at high energies, the cross sections of ^{150}Dy and ^{151}Dy are nearly equal. Moreover the production threshold of ^{150}Dy is slightly higher than that of ^{151}Dy. Therefore, the cross sections measured for ^{150}Dy can be taken as upper limits for the production of ^{149}Dy. Multiplying these values by r, one obtains the dotted line shown in fig. 2. From the comparison of this curve with the measured excitation function of ^{149g}Tb, it seems clear that the high energy part of the ^{149g}Tb excitation function can be essentially assigned to the term $r\,\sigma(^{149}Dy)$. On the other hand, the difference observed between the low energy cross sections may be attributed to the direct production of ^{149g}Tb.

It should be emphasized that the measured cross section for ^{149g}Tb is different from the cumulative yield for ^{149}Tb, which includes the contribution of ^{149m}Tb. Otherwise, one would expect the corresponding excitation function to be continuously increasing, as it is generally observed for transfer reactions.

The excitation functions for all the reactions studied are shown in figs 3 and 4. It can be seen in fig. 3 that the effect mentioned for the reaction $^{40}Ar + ^{144}Sm$ is also observed, but less clearly, for the reaction $^{40}Ar + ^{142}Nd$ for $E_{lab} \leq 200$ MeV. For the other reactions, the excitation functions of which are drawn in solid lines in fig. 3, the effect does not appear. But one should remark that, because of their low values, the cross sections corresponding to these reactions have not been measured for $E_{lab} \leq 200$ MeV. The conclusion therefore is that ^{149g}Tb can be produced directly with non negligible cross sections in Ar induced reactions when the incident energy is lower than 200 MeV.

As far as Cu induced reactions are concerned, it can be seen in fig. 4 that the same features are observed : the curves corresponding to ^{150}Dy and ^{151}Dy exhibit similar shapes while that for ^{149g}Tb is somewhat different. There again the magnitude of the cross section for ^{149g}Tb is about twice less than that for ^{150}Dy at high energy, and becomes significantly higher at low energy. This behaviour is consistent with the hypothesis that the main contribution to the observed cross section for ^{149g}Tb is the E.C. decay of ^{149}Dy at high energy, and the direct production of ^{149g}Tb for $E_{lab} \lesssim 325$ MeV.

III - INTERPRETATION IN TERMS OF Tb FRAGMENT ANGULAR MOMENTA

Generally, a deep inelastic reaction is described as follows : the incident nuclei approach each other, and when they come in contact, exchange several nucleons. Simultaneously there is a loss of kinetic energy due to radial friction, and a transformation of orbital angular momentum into intrinsic angular momentum. After separation there are two main fragments, each one having an excitation energy E^* and a spin J. Then the fragments evaporate particles and emit γ rays to give the cold nuclei. Such cold nuclei, or their radioactive daughters, are observed in the present experiments.

If one neglects the deformation effects, the deexcitation of an excited Dy or Tb fragment, after separation from the light one, can be treated in the same way as that of an identical nucleus produced through a fusion reaction, the only possible difference being the initial population of excitation energy E^* and angular momentum J. The excitation energies of the Tb fragments produced in the present experiment can be calculated from the kinetic energy measured for the Tb residues, assumming a two-body process and a sharing of the excitation energies between the fragments proportionnally to their masses[8-10]. Such calculations lead to E^* values lying in the range 30-60 MeV according to the incident energy for the projectiles ^{40}Ar and ^{63}Cu. The results of Alexander and Simonoff[11] concerning the residual nuclei produced through compound nucleus reactions in the rare earth region have shown that :

i) in the range of excitation energy concerned here, the rare earth nuclei deexcite mainly (95 %) through neutron evaporation, followed by γ-ray emission. Calculations using the Grogi code [17] for Dy and Tb nuclei give the same result.

ii) as far as ^{149g}Tb residual nuclei are concerned, only those Tb nuclei of angular momentum J_{Tb} lower than a given angular momentum cut-off J_c lead, after deexcitation, to this low spin isomer, whatever the excitation energy is. The compound nuclei of angular momenta higher that J_c produced, after deexcitation, the high spin isomer ^{149m}Tb. This isomer was not observed in these experiments. Over a wide range of Tb excitation energies (from 40 to 110 MeV), the value found for J_c appeared to be independant of E^*, and equal to $7.5 \pm 1.5\,\hbar$.

One should note here that the absolute value of the angular momentum cut-off depends on the α branching ratios adopted for the observed isotopes $^{150,151}Dy$ and ^{149g}Tb. Since the work of ref.[11], new determinations of these ratios have been performed, and the values generally adopted now are somewhat different from those taken in ref.[11] (see table 1). It has been checked, however, that the resulting variation of the angular momentum cut-off was smaller than the given uncertainty. Therefore, the condition

$$J_{Tb} < 7.5 + 1.5 = 9\,\hbar \qquad (3)$$

which takes into account the uncertainty in J_c will be retained henceforth as necessary for a Tb excited nucleus to produce, through deexcitation, a ^{149g}Tb residue with a high probability.

This condition can be applied to the present data, and the shapes observed for the Tb excitation functions may now be interpreted as an evidence that for low incident energies (E_{lab}(Ar) < 200 MeV and E_{lab}(Cu) < 325 MeV), a significant fraction of the Tb fragments from DIT are produced with angular momenta lower than 9 $\hbar$.

It is very important to notice that this result is relative to primary fragments produced in the first step of the transfer reaction, i.e., before deexcitation.

IV - CONSEQUENCES RELATIVE TO THE REACTION MECHANISM

Two types of hypothesis are needed to calculate the angular momentum of DIT fragments. The first one concerns the initial partial waves ℓ_i leading to D.I.T. reactions : according to the model mostly adopted, these partial waves correspond to a region situated between the critical angular momentum for fusion, ℓ_{cr}, [18] and the grazing angular momentum ℓ_{gr} associated with quasi-elastic reactions. This hypothesis will be adopted here.

The second type of hypothesis is required to calculate the fraction of the initial angular momentum which is transformed into intrinsic angular momentum of the fragments, and its sharing between them at scission. This hypothesis concerns the relative rotation of the nuclei during their contact : the assumptions of rolling or sticking fragments are generally adopted as defining the extreme possible situations (see below and ref.[19]).

In what follows, the intrinsic angular momentum of Tb fragments J_{Tb} will be calculated, for the relevant incident energies and ions using the assumption $\ell_{cr} < \ell_1 < \ell_{gr}$, and the rolling and sticking models. The range of values obtained for J_{Tb} will then be compared, for each incident energy, to the results previously derived from the experimental data.

IV.1. Principle of the calculation

No experimental data are available for the critical angular momentum ℓ_{cr} corresponding to the systems studied here. Therefore, this value has been determined using the concept of "critical distance" which was developed some years ago[18] and is in good agreement with many experimental values of the fusion cross section. The nuclear potential used in this calculation is derived from the energy density formalism[20].

The value ℓ_{gr} is calculated by the approximation

$$\ell_{gr}\hbar = (R_1 + R_2)\,[2\mu(\bar{E} - \bar{B})]^{1/2} \qquad (4)$$

where R_1 and R_2 are the nuclear radii of the incident nuclei, μ is the reduced mass, and $\bar{B}$ the c.m. interaction barrier. It will be seen, however, that the exact value of ℓ_{gr} has little influence on the following discussion, the main parameter being ℓ_{cr} which determines the lower limit for J_{Tb}.

The transformation of the initial orbital angular momentum into intrinsic angular momentum of the fragments is attributed, in classical models, to the tangential friction. Generally this force is divided into sliding friction which develops against the sliding motion, and rolling friction which acts against rolling. In a rather rough simplification, two limiting situations are considered[19] :

- In the hypothesis of rolling, which corresponds to the earlier stage of the reaction , the two nuclei roll over each other without sliding. If spherical shapes are assumed for these nuclei, the angular momentum J transferred to the fragments is independent of their masses, and is equal to $J_r = 2/7\ \ell_i$. It is then shared between the fragments proportionally to their nuclear radii.

- In the hypothesis of sticking, which corresponds to a later stage, the two nuclei are supposed to be rigidly bound, as if they were stuck. Their rotation is then similar to that of a rigid body, and J gets its maximum value :

$$J_s = \ell_i \frac{\mathcal{J}_\ell + \mathcal{J}_h}{\mu R^2 + \mathcal{J}_\ell + \mathcal{J}_h} \qquad (5)$$

where $\mathcal{J}_\ell$ and $\mathcal{J}_h$ are the moments of inertia of the light and heavy fragments, respectively, considered as spherical ; μ is the reduced mass of the composite system and R is the distance of the two fragments centers before scission. As the composite system is certainly very deformed, it has been considered as made of two spheres, the centers of which are separated by a distance $R_\ell + R_h + d$, with $R_{\ell,h} = 1.22\ A_{\ell,h}^{1/3}$. The value chosen for the parameter d(d = 6 fm) has been determined using the experimental kinetic energies measured for the heavy fragment of the studied reactions[14]. It should be noted that this value is somewhat higher than those resulting from other studies, and this may lead to an overestimation of R , i.e. to an underestimation of J_s. At scission, the angular momentum J_s is shared between the fragments proportionally to their moments of inertia.

IV.2. Results

The angular momenta J_{min} and J_{max} of the Tb fragments, corresponding respectively to the extreme values (ℓ_{cr} and ℓ_{gr}) of ℓ_i, have been calculated using the sticking and the rolling hypothesis. The results obtained for the systems $^{63}Cu + {}^{148}Sm$, and $^{40}Ar + {}^{144}Sm$ are presented in tables 5 and 6, for various incident energies. For a given incident ion, similar results would be obtained for the other targets, as a slight change in the target mass does not influence much the calculated angular momenta. If an uncertainty of ± 15 % is assumed in the value of ℓ_{cr}, the error on J_{min} values is certainly higher because of the additional uncertainties involved in the calculation (mass of the fragments, moments of inertia of the composite system and of the fragments). It has been estimated to be around ± 30 %.

The results summarized in table 5 and 6 can be interpreted as follows :

IV.2.1. System $^{63}Cu + ^{148}Sm$:

The calculated values of J_{min} and J_{max} do not depend on the hypothesis made about rolling or sticking. This can be explained by the combination of two effects :

i) the introduction of a separation distance d=6fm lowers the value J_s below the value $J_r = 2/7\ \ell_i$,

ii) the relative values of the fragment masses and radii are such that the previous effect is almost exactly compensated by the angular momentum sharing.

It is remarkable to observe in table 5 that, for the lowest incident energies, most of the Tb fragments are produced with angular momenta lower than 9 $\hbar$, while, on the other hand, the calculated J_{Tb} interval corresponds to much higher values when the incident energy is high. This result is in excellent agreement with the experimental observation, i.e. an enhancement of the production yield for ^{149g}Tb at low energy. Even the experimental transition energy of about 325 MeV is well accounted for by the calculation, as it corresponds to the energy above which the calculated J_{Tb} excludes the values lower than 9 $\hbar$.

IV.2.2. System $^{40}Ar + ^{144}Sm$:

It can be seen in table 6 that, if the sticking hypothesis is made, the range of possible values of J_{Tb} ($J_{min} \leq J_{Tb} \leq J_{max}$) never allows J_{Tb} values lower than 9 $\hbar$. This means that the direct production of ^{149g}Tb at low energy cannot be explained with this hypothesis. On the other hand, if the hypothesis of rolling is adopted, the calculated values of J_{min} become lower than 9 $\hbar$ for $E_{lab}(Ar) \lesssim 190$ MeV. If one takes into account the uncertainty of ± 30 % on these values, these results are also in agreement with the experimental transition observed at $E_{lab}(Ar) \approx 200$ MeV, an energy for which $J_{min} = 11 \pm 3\ \hbar$.

Therefore, for Ar induced reactions, the experimental observations can only be interpreted under the assumption that the scission occurs while the fragments are still in the stage of rolling, at least for incident energies lower than 200 MeV. As far as higher incident energies are concerned, both hypothesis, sticking or rolling, lead to J_{Tb} intervals excluding values lower than 9 $\hbar$, and are therefore consistent with very low production yields for ^{149g}Tb. Consequently, no selection between these two models can be made from the present data, at high energy.

IV.3. Discussion

From the previous section, it can be concluded that the experimental observations are in good agreement with the intrinsic angular momenta for Tb fragments that may be calculated under the hypothesis mentioned. It is particularly encouraging that the calculations lead to angular momenta lower than 9 $\hbar$ in the proper energy region for both projectiles, and at least for one of the hypothesis, rolling or sticking. However, it seems worthwhile to dicuss (i) the choice of the initial angular momentum window, (ii) the influence of the parameter d, and (iii) the physical meaning of the rolling assumption.

The initial angular momentum window which has been chosen corresponds to the usual picture according which the deep inelastic transfer reactions are intermediate between complete fusion and quasi-elastic reactions. It has however been suggested[21-23] that at least part of these reactions could be produced for low impact parameters, below an hypothetic lower critical angular momentum for fusion. As there is no clear experimental evidence for the existence of this low critical angular momentum, and without any indication about its possible values and variation versus incident energy, it was difficult to perform any calculation using such hypothesis. One should however remark that the use of low ℓ_1 values would certainly lead to J_{Tb} values lower than 9 $\hbar$, i.e., to some production of ^{149g}Tb for all incident energies.

The value d = 6 fm adopted in the hypothesis of sticking may seem to be high when compared to other values which have been reported[24,25] But one should remark that the present value has been calculated in order to fit the observed kinetic energies of residual nuclei, taking into account the centrifugal term which results from the angular momentum of fragments, while this term is often neglected. This may explain a difference of about 1 fm in favour of the present value. Secondly, as was outlined in ref.[10,14] the distance d depends on the ratio E/B of the incident energy to the interaction barrier. In any event, the conclusions relative to the validity of the sticking or rolling hypothesis remain the same for both projectiles (Ar and Cu) even if the value of d is significantly decreased : As far as the Ar induced reactions are concerned, this results in an increase of the J_{Tb} value calculated in the hypothesis

of sticking, and the hypothesis of rolling remains the only valid one. For Cu induced reactions, if the value of d is taken equal to 3 fm, which seems a reasonable lower limit, the J_{Tb} values increases by 33 %, and still the distribution between rolling and sticking cannot be made because of the uncertainties involved in the calculation.

Finally, one should remark that the hypothesis of rolling is difficult to reconcile with a strong deformation of the composite system at scission. For the angular momentum calculations, it has been associated with the hypothesis of two tangent spheres. But this leads to kinetic energies higher by 50 % than those calculated with d = 6 fm, which correspond to the mean kinetic energies observed for heavy fragments at incident energies E_{lab}(Cu) = 330 and 420 MeV, i.e. for E/B = 1.15 to 1.4 [14]. As the value of d increases when E/B decreases, one may expect that, close to the barrier, the mean kinetic energy of Dy fragments is even lower. But, in the absence of kinetic energy measurements at the relevant energies, one cannot exclude the possibility that the ^{149g}Tb fragments produced for energies close to the interaction barriers correspond to reactions in which the kinetic energy is not totally damped. Another explanation of this apparent contradiction between the kinetic energy data and the validity of the hypothesis of rolling would be that the stage of rolling represents an extreme situation, which is convenient for calculating limits for the possible angular momentum transfers, but non realistic. The nuclei are not rigid bodies, and the composit system may lie between this rolling limit and the opposite limit of sticking, which is probably more realistic. Therefore, the present conclusion concerning Ar induced reactions below 200 MeV should be expressed by saying that the stage of sticking is not reached before the scission of the composite system.

V - SUMMARY AND CONCLUSION

The low energy enhancements observed in the excitation functions for ^{149g}Tb production through various DIT reactions have been attributed to the direct production of this low spin isomer, while the high energy parts of the excitation functions are mainly due to the decay of ^{149}Dy. Using results from (heavy ion,xn) reactions, this direct production can be interpreted as an evidence for the existence of primary fragments of angular momenta lower than 9 ħ. From the general pattern of ^{149g}Tb excitation functions, it is therefore deduced that Tb fragments of intrinsic

angular momenta lower than 9 $\hbar$ are produced with significant probabilities for $E_{Ar} \lesssim 200$ MeV and $E_{Cu} \lesssim 325$ MeV.

These data appear to be in very good agreement with the angular momenta calculated for Tb fragments under the hypothesis that those initial angular momenta which lead to DIT reactions are situated between the critical angular momentum for fusion ℓ_{cr} and the value ℓ_{gr} corresponding to quasi-elastic events. As far as Cu projectiles are concerned, the hypothesis of rolling and sticking fragments at scission lead to the same angular momenta for Tb fragments, and both agree with the experimental data. On the other hand, the data concerning Ar induced reactions indicate that, for low incident energies, the fragments separate from each other before the stage of sticking is reached. The same conclusion was obtained in ref.[26] for the Ar + Au reaction at 227 MeV (i.e., slightly over the interaction barrier) on the basis of gamma multiplicity and gamma energy measurements. On the contrary, for incident energies well above the interaction barrier, it was deduced from other experiments[4,27,28] that the stage of sticking was achieved. These two sets of conclusions may not exclude each other, because it is possible, as suggested by Moretto and Schmitt[29] for the interpretation of experimental DIT mass distributions, that the life-time of the composite system increases with incident energy.

We thank the ALICE crew for their cooperation, M. Lefort and J.M. Alexander for careful reading of the manuscript.

REFERENCES

[1] A. Albrecht, W. Dunnweber, G. Graw, H. Ho, S.G. Steadman and J.P. Wurm, Phys. Rev. Lett. 34, 1400 (1975).

[2] H. Ishihara, T. Numao, T. Fukuda, K. Tanaka and T. Inamura, IPCR-cyclotron report 35, Contribution to the Argonne Symposium (1976).

[3] M. Berlanger, M.A. Deleplanque, C. Gerschel, F. Hanappe, M. Leblanc, J.F. Mayault, C. Ngô, D. Paya, N. Perrin, J. Péter, B. Tamain and L. Valentin, Conf. Eur. Phys. avec Ions Lourds, Caen (1976), p. 173

[4] P. Dyer, R.J. Puigh, R. Vandenbosch, T.D. Thomas and M.S. Zisman, Phys. Rev. Lett. 39, 392 (1977).

[5] T.M. Cormier, P. Braun-Munzinger, P.M. Cormier, J.W. Harris and L.L. Lee Jr., Phys. Rev. C16, 215 (1977).

[6] W. Trautmann, J. de Boer, W. Dünweber, G. Graw, R. Kopp, C. Lauterbach, H. Puchta and U. Lynen, Phys. Rev. Lett. 39, 1062 (1977).

[7] K. Tanaka, M. Ishihara, H. Kamitsubo, N. Takahashi, A. Mizobuchi, Y. Nojiri, T. Minamisono and K. Sugimoto, Phys. Rev. Lett. 39, 323 (1977).

[8] R. Bimbot, D. Gardès, R.L. Hahn, Y. De Moras and M.F. Rivet, Nucl. Phys. A228, 85 (1974).

[9] R. Bimbot, D. Gardès, R.L. Hahn, Y. de Moras and M.F. Rivet, Nucl. Phys. A248, 377 (1975).

[10] M.F. Rivet, R. Bimbot, A. Fleury, D. Gardès and Y. Llabador, Nucl. Phys. A276, 157 (1977).

[11] J.M. Alexander and G. Simonoff, Phys. Rev. 130, 2383 (1963).

[12] R. Bimbot, S. Della Negra, D. Gardès, H. Gauvin and B. Tamain, IPNO-RC-77-03, Rev. Phys. Appl. 13 , 393 (1978).

[13] R. Bimbot, S. Della Negra, D. Gardès, H. Gauvin, A. Fleury and F. Hubert, Nucl. Instr. Meth. 153, 161 (1978).

[14] M.F. Rivet, Thesis, Orsay (1977), unpublished

[15] C. Ngô, B. Tamain, J. Galin, M. Beiner, and R.J. Lombard, Nucl. Phys. A240, 353 (1975).

[16] H. Gauvin, R.L. Hahn, B. Lagarde, Y. Le Beyec, M. Lefort, C.R. Acad. Sc. Paris, 277 (1973) p. 107.

[17] H. Delagrange, F. Hubert and A. Fleury, Nucl. Phys. A228, 397 (1974)

[18] J. Galin, D. Guerreau, M. Lefort and X. Tarrago, Phys. Rev. C9, 1018 (1974).

[19] M. Lefort and C. Ngô, Ann. Phys. 3, 5 (1978).

[20] C. Ngô, B. Tamain, M. Beiner, R.J. Lombard, D. Mas and H.H. Deubler, Nucl. Phys. A252, 237 (1975).

[21] M. Lefort, Phys. Scripta, 10A, 90 (1974).

[22] R. Broglia et al. (unpublished data).

[23] K. Siwek-Wilczinska and J. Wilczinsky, Nucl. Phys. A264, 115 (1976).

[24] B. Gatty, D. Guerreau, M. Lefort, J. Pouthes, X. Tarrago, J. Galin, B. Cauvin, J. Girard and H. Nifenecker, Z. Phys. A273, 65 (1975) ; Nucl. Phys. A253, 511 (1975).

[25] R. Babinet, L.G. Moretto, J. Galin, R. Jared, J. Moulton and S.G. Thompson, Nucl. Phys. A258, 172 (1976).

[26] M.A. Deleplanque, C. Gerschel, M. Ishihara, C. Ngô, N. Perrin, J. Péter, B. Tamain, L. Valentin, D. Paya, Y. Sugiyama, M. Berlanger and F. Hanappe, Communication to the Meeting on Heavy Ion Collisions, Pikeville, U.S.A. (1977).

[27] P. Glässel, R.S. Simon, R.M. Diamond, R.C. Jared, I.Y. Lee, L.G. Moretto, J.O. Newton, R. Schmitt and F.S. Stephen, Preprint XBL 7611-4446 (1976).

[28] J.B. Natowitz, M.N. Namboodiri, P. Kasiray, R. Eggers, L. Ader, P. Gouthier, C. Cerruti and T. Alleman (unpublished data).

[29] L.G. Moretto and R. Schmitt, Conf. Europ. Phys. Ions Lourds, J. Phys. C5, 109 (1976).

[30] C.R. Bingham, D.U. O'Kain, K.S. Toth and R.L. Hahn, Phys. Rev. C7, 2575 (1973).

[31] R.D. Mac Farlane and D.W. Seegmiller, Nucl. Phys. 53, 449 (1964).

[32] J.O. Rasmussen, S.W. Thompson and A. Ghiorso, Phys. Rev. 89, 33 (1953).

TABLE CAPTIONS

Table 1 : Characteristics of the observed isotopes. The symbol EC denotes a decay through electron capture. The branching ratios adopted here are denoted R, those adopted in ref.[11] are denoted R(Ref.[11]).

Table 2 : Transfer reactions leading from each target to each residual nucleus. The net gain of nucleons by the target given for each reaction is the balance of the two steps : transfer + evaporation.

Table 3 : Experimental cross sections for Ar induced reactions.

Table 4 : Experimental cross sections for Cu induced reactions.

Table 5 : Calculated limits for the intrinsic angular momentum of excited Tb fragments under the assumptions of sticking and rolling behaviors of the composite system, for the reaction $^{63}Cu + ^{148}Sm$. The quantities ℓ and J are given in $\hbar$ units.

Table 6 : Same as table 5, for the reaction $^{40}Ar + ^{144}Sm$.

TABLE 1

Isotope	$T_{1/2}$	E_α (MeV)	R	Ref.	R(Ref.[11])
^{149g}Tb	4.1 h	3.96	0.16±0.04	30	0.10
^{150}Dy	7.2 mn	4.23	0.32±0.03	31	0.179
^{151}Dy	18 mn	4.06	0.06±0.006	32	0.062
^{149}Dy	15 mn	EC	0.475±0.05[1]	16	0.33[1]

[1]Branching ratio for the EC decay of ^{149}Dy leading to ^{149g}Tb

TABLE 2

Target	Produced isotope			
	^{151}Dy	^{150}Dy	^{149}Dy	^{149}Tb
^{142}Nd	+6p+3n	+6p+2n	+6p+n	+5p+2n
^{144}Nd	+6p+n	+6p	+6p-n	+5p
^{145}Nd	^6p	+6p-n	+6p-2n	+5p-n
^{144}Sm	+4p+3n	+4p+2n	+4p+n	+3p+2n
^{148}Sm	+4p-n	+4p-2n	+4p-3n	+3p-2n
^{151}Eu	+3p-3n	+3p-4n	+3p-5n	+2p-4n
^{154}Gd	+2p-5n	+2p-6n	+2p-7n	+p-6n

TABLE 3

Projectile : ARGON

^{142}Nd target

E (MeV)	Cross sections (mb)		
	^{151}Dy	^{150}Dy	^{149g}Tb
292.6	2.7 ± .4	2.4 ± .4	.80 ± .12
275.3	2.30± .45	1.42 ± .35	.45 ± .15
247.4	.92± .18	.38 ± .09	.06 ± .02
220.8	.23± .12	.05 ± .02	.016 ± .008
217.8	.13± .02	0.02 ± .003	.012 ± .002
202.9	<.02	< .02	≤ .02
180.3	.012±.003	.0002±.0001	.005 ± .002

^{145}Nd target

E (MeV)	^{151}Dy	^{150}Dy	^{149g}Tb
274.9	1.45± .29	.50 ± .12	.10 ± .03
246.9	.21± .04	.09 ± .02	.039 ± .007
214.0	< .01	< .003	< .003

^{144}Sm target

E (MeV)	^{151}Dy	^{150}Dy	^{149g}Tb
277.1	4.8 ±.8	4.8 ±.8	2.21 ± .26
240.9	3.5 ±.8	3.8 ±.7	1.53 ± .44
221.6	2.2 ±.6	1.55 ±.33	.94 ± .22
218.7	2.25 ±.33	1.31 ±.22	.33 ± .05
203.0	1.2 ±.2	.55 ±.09	.17 ± .03
180.4	.27 ±.04	.087±.015	.15 ± .02
162.5	.036±.014	.015±.004	.055± .013

^{148}Sm target

E (MeV)	^{151}Dy	^{150}Dy	^{149g}Tb
276.1	4.5 ±.8	1.70 ±.34	.38 ± .08
242.2	1.8 ±.45	.37 ±.09	.170± .045
218.5	.12 ±.02	.040±.007	.030± .006
218.2	.14 ±.02	.037±.010	.014± .002
198.2	.013±.004	.017±.004	.004± .001

^{154}Gd target

E (MeV)	^{151}Dy	^{150}Dy	^{149g}Tb
273.3	2.34 ±.42	.88 ± .16	.20 ± .04
212.6	.03 ±.01	.022 ± .006	.005 ± .001
196.7	.004±.002	.006 ± .002	.007 ± .001
177.9	-	< .003	< .003

TABLE 4

Projectile : COPPER

^{144}Nd target	Cross sections (mb)		
E (MeV)	^{151}Dy	^{150}Dy	^{149g}Tb
421.3	5.7 ±1.1	7.1 ± 1.5	2.8 ±.6
400.4	4.8 ± .9	4.1 ± .6	1.7 ±.3
361.8	1.8 ± .5	1.60± .25	.57 ±.11
332.7	.91 ± .16	.41± .07	.17 ±.02
310.7	.16 ± .16	.13± .06	.086±.023
285.4	< .08	< .02	<.05

^{148}Sm target

E (MeV)	^{151}Dy	^{150}Dy	^{149g}Tb
422.4	17.1 ±2.7	15.7 ±2.7	6.3 ±1.0
422.4	18.0 ±3.0	14.4 ±2.4	6.6 ±1.1
402.3	14.2 ±2.4	8.9 ±1.5	4.8 ± .8
363.8	4.65 ± .90	3.85 ± .55	2.0 ± .3
330.3	3.20 ± .46	1.14 ± .17	.75± .11
312.7	1.40 ± .25	.37 ± .06	.44± .08
267.1	.045± .045	.022± .016	.12± .08

^{151}Eu target

E (MeV)	^{151}Dy	^{150}Dy	^{149g}Tb
416.1	16.6 ±2.4	11.6 ±1.8	5.2 ±.8
401.6	11.6 ±1.9	9.0 ±1.4	3.7 ±.5
362.9	7.4 ±1.1	3.6 ± .5	1.6 ±.2
328.0	3.1 ± .4	1.3 ± .2	.64 ±.1
312.0	1.11 ± .18	.31 ± .07	.31 ±.05
286.7	< .17	< .045	.056±.022

^{154}Gd target

E (Mev)	^{151}Dy	^{150}Dy	^{149g}Tb
398.6	13.1 ±2.4	6.6 ±1.5	3.3 ± .7
359.8	5.2 ± .8	3.0 ± .4	1.3 ± .2
308.7	.65 ± .10	.20 ± .04	.15± .02
293.8	.16 ± .03	.04 ± .01	.07± .02
283.3	.04 ± .04	.005± .005	.018±.018

TABLE 5

$^{63}Cu + {}^{148}Sm$

E_{lab} (MeV)	ℓ_{i}^{cr}	ℓ_{i}^{gr}	J_{Tb}(sticking)		J_{Tb}(rolling)	
			J_{min}	J_{max}	J_{min}	J_{max}
400	112	150	19±6	26±9	19±6	26±9
350	76	113	13±4	19±6	13±4	19±6
330	60	90	10±3	15±5	10±3	15±5
320	48	76	8±3	13±4	8±3	13±4
310	33	59	5±2	10±3	5±2	10±3

TABLE 6

Ar + ^{144}Sm

E_{lab} (MeV)	ℓ_i^{cr}	ℓ_i^{gr}	J_{Tb}(sticking)		J_{Tb}(rolling)	
			J_{min}	J_{max}	J_{min}	J_{max}
300	111	150	32±11	43±14	20±7	27±9
250	90	118	26±9	34±11	16±5	21±7
225	76	98	22±7	28±9	14±5	17±6
200	60	73	17±6	21±7	11±4	13±4
195	57	66	16±5	13±6	10±3	12±4
190	53	60	15±5	17±6	9±3	11±4
185	48	52	14±5	15±5	8±3	9±3

FIGURE CAPTIONS

Figure 1 : Excitation functions for the reactions $^{40}Ar + {}^{144}Sm \rightarrow {}^{151}Dy$ (stars), ^{150}Dy (circles) and ^{149g}Tb (triangula). The cross sections are plotted versus the incident energy in the lab system (E_{lab}) and in the c.m. system ($\bar{E}$). The curves are drawn to guide the eye. The arrow indicates the interaction barrier, calculated from ref.[15].

Figure 2 : Comparison of the excitation functions for the production of ^{150}Dy and ^{149g}Tb through $^{40}Ar + {}^{144}Sm$. The triangles are the experimental points measured for ^{149g}Tb, the solid line is drawn to guide the eye. The circles and the dotted line represent the cross section of ^{150}Dy multiplied by r (see text) and can be interpreted as an upper limit for the contribution of the ^{149}Dy decay in the production of ^{149g}Tb.

Figure 3 : Excitation functions for ^{40}Ar induced reactions.
a) six charge transfers,
b) four charge transfers,
c) two charge transfers.
(same symbols as in fig. 1).

Figure 4 : Excitation functions for ^{63}Cu induced reactions.
a) six charge transfers,
b) four charge transfers,
c) three charge transfers,
d) two charge transfers.
(same symbols as in fig. 1). The dotted lines have the same meaning as in fig. 2 (i.e., $r.\sigma\ (^{150}Dy)$).

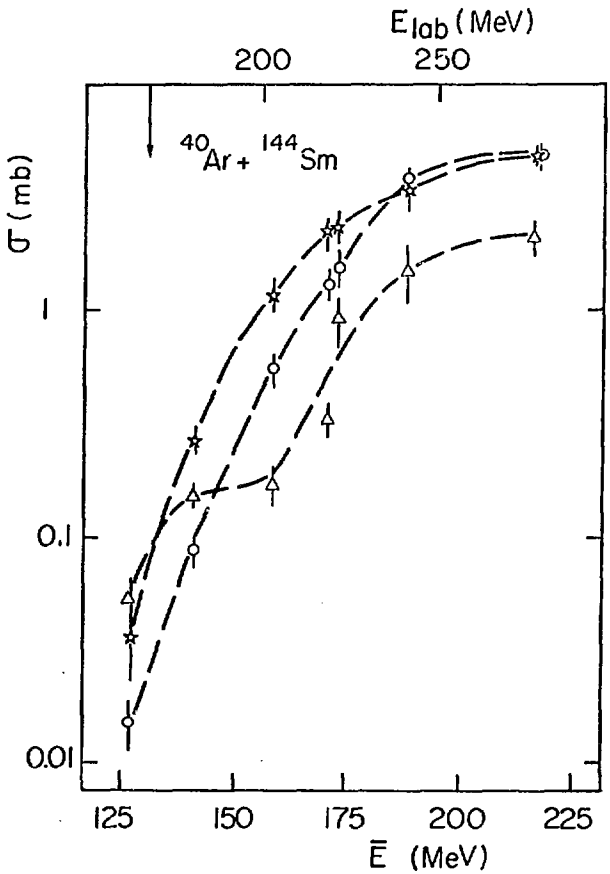
E lab (MeV)
200
250
40Ar + 144Sm
σ (mb)
1
0.1
0.01
125
150
175
200
225
Ē (MeV)

Figure 1

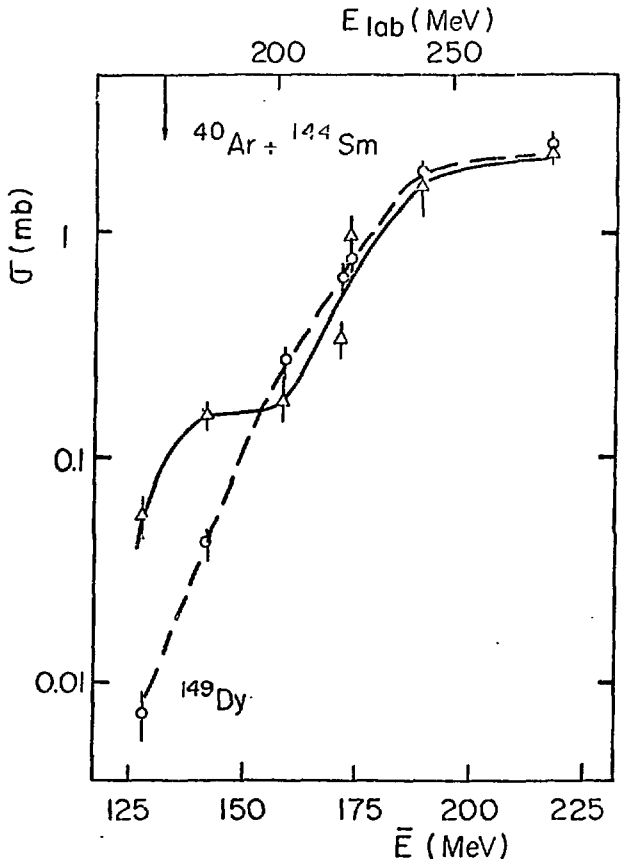
E lab (MeV)
200
250
40Ar + 144Sm
σ (mb)
1
0.1
0.01
149Dy
125
150
175
200
225
Ē (MeV)

Figure 2

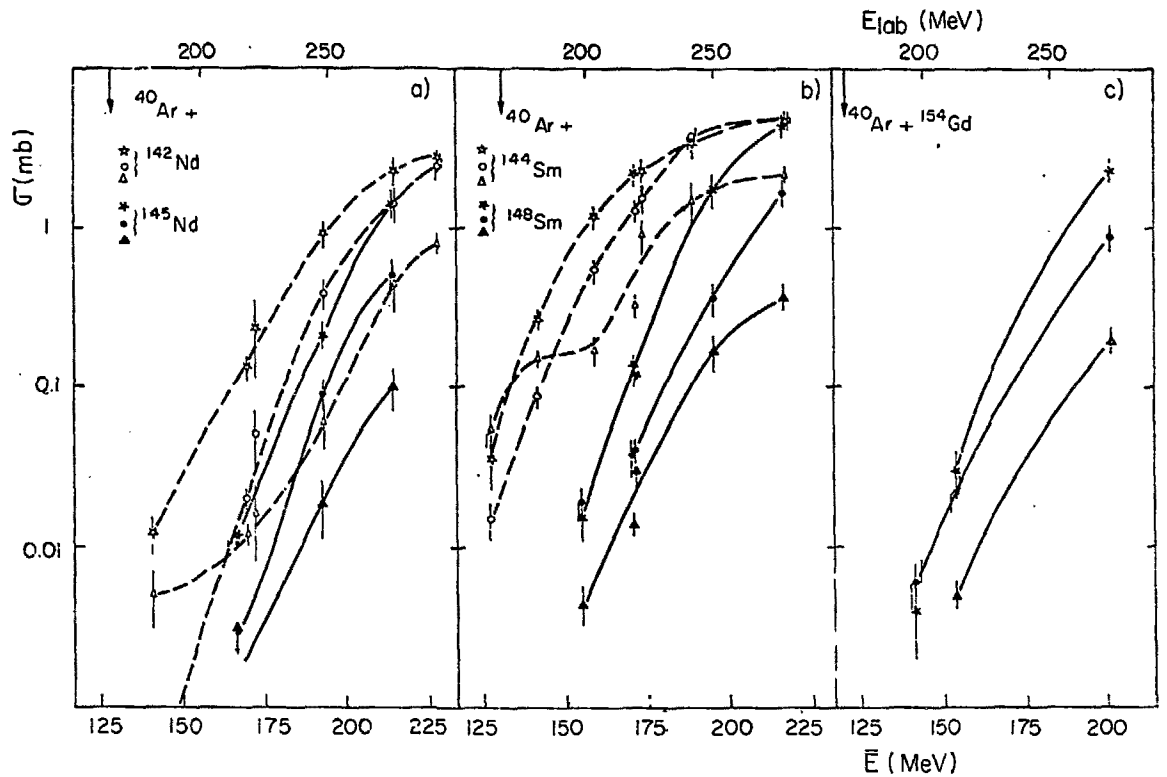
Elab (MeV)
200
250
a)
b)
c)
40Ar +
142Nd
145Nd
144Sm
148Sm
154Gd
σ(mb)
1
0.1
0.01
125
150
175
200
225
Ē (MeV)

Figure 3

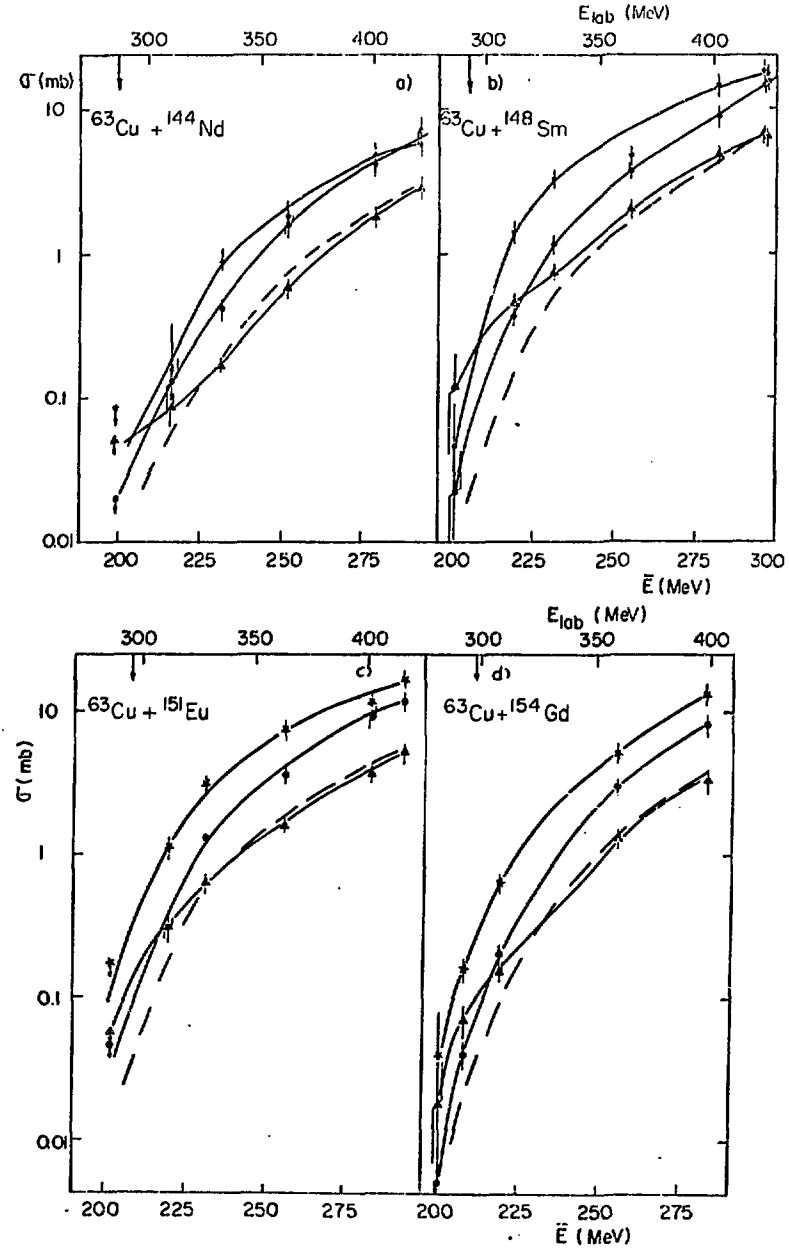
E_lab (MeV)
300
350
400
σ (mb)
10
1
0.1
0.01
a)
63Cu + 144Nd
b)
63Cu + 148Sm
200
225
250
275
300
Ē (MeV)
c)
63Cu + 151Eu
d)
63Cu + 154Gd

Figure 4